

# Cu-Ln (Ln = Gd, Eu, Sm) Dinuclear Complexes Based on Schiff Base *o-van-en* Ligand: Syntheses, Crystal Structures, and Magnetic Properties

Andrea Koščíková,<sup>[a]</sup> Juraj Černák,<sup>\*[a]</sup> Larry R. Falvello,<sup>[b]</sup> Milagros Tomás,<sup>[c]</sup> Irene Ara,<sup>\*[c]</sup> Ján Titiš,<sup>[d]</sup> and Roman Boča<sup>[e]</sup>

Three new dinuclear complexes [CuCl(*o-van-en*)Ln(H<sub>2</sub>O)<sub>3</sub>Cl]Cl·C<sub>2</sub>H<sub>6</sub>O (Ln = Sm (1), Eu (2), Gd (3); H<sub>2</sub>(*o-van-en*) is the Schiff base formed by 2/1 condensation of *o*-vanillin and ethylenediamine) were prepared in a single crystal form by the method of horizontal diffusion. The prepared complexes were characterized by chemical analyses and IR spectroscopy. The three complexes are isostructural and the Cu(II) is situated in the smaller cavities

while the larger cavities accommodate larger Ln(III) atoms. The pentacoordination of the Cu(II) atoms is completed by a chlorido ligand in the apical position, while the octacoordination of the Ln(III) atoms is achieved by three additional aqua and one chlorido coligands. AC susceptibility studies have shown that complexes 2 and 3 exhibit field supported slow magnetic relaxation while complex 1 does not display AC activity.

## 1. Introduction

In recent years, the demand for new magnetic materials that can be used to store large amounts of data has been steadily increasing.<sup>[1]</sup> Single-molecule magnets (SMM) are molecules that exhibit slow magnetic relaxation and single-ion magnets (SIM) form part of this group. There are different parameters that define the magnetic relaxation barrier of SMMs such as the total spin (*S*) and the axial anisotropy (*D*). Lately there has been

major interest in studying lanthanides mainly for their spin-orbit coupling influence on the ground electronic state. Sandwich like complexes were the first to exhibit interesting magnetic properties.<sup>[2]</sup>

Transition metal–lanthanide bimetallic complexes (3*d*–4*f* type) are also suitable candidates for such studies because they combine magnetic properties of both central atoms.<sup>[3]</sup> The influence of the chosen lanthanide, the volume, and properties of the ligand and solvent are important considerations. Stability and lanthanide contraction play interesting roles in the preparation of magnetically active complexes. The aqua ligands combined with halide ligand create asymmetry, which is crucial for slow magnetic relaxation. It should also be mentioned that the major part of the studies conducted to date were made on complexes containing the (NO<sub>3</sub>)<sup>−</sup> ligand, as those are quite easy to prepare.<sup>[4]</sup>

Complexes containing [Cu(*o-van-en*)] with nitrate ligands or nitrate counterions are those most represented in the literature. As an example, it is possible to mention [Cu(*o-van-en*)Sm(NO<sub>3</sub>)<sub>2</sub>(H<sub>2</sub>O)<sub>2</sub>](NO<sub>3</sub>).<sup>[5]</sup> Two complexes have hexafluoroacetylacetonato ligand.<sup>[6]</sup> Only one of the coordination compounds contains chlorido ligand bonded to the lanthanide atom, namely [CuCl(*o-van-en*)Tb(H<sub>2</sub>O)<sub>3</sub>Cl]Cl·CH<sub>3</sub>OH (SAXVOE).<sup>[7]</sup>

Previously, it was shown that in [Ni(*o-van-en*)Gd(H<sub>2</sub>O)Cl<sub>3</sub>] the presence of diamagnetic Ni(II) atoms and/or asymmetric coordination of the three chloride ligands induced anisotropy in the Gd(III) atom and a field induced slow magnetic relaxation was observed.<sup>[8]</sup> It is interesting to note that recently it was reported that such 3*d*–4*f* complexes can be prepared by using an asymmetric bicompartamental ligand based on a combination of ethylenediamine, *o*-vanillin, and salicylaldehyde.<sup>[9]</sup> All these findings inspired us to further investigate complexes of this type.

It is well known that the ground state of Eu(III) (<sup>7</sup>F<sub>0</sub>) is diamagnetic but upon heating the thermally excited multiplets become populated and the Eu center becomes magnetically active. Despite this, in the complex Eu(*Rad*) (NO<sub>3</sub>)<sub>3</sub>] (*Rad* is

[a] A. Koščíková, Prof. Dr. J. Černák  
Department of Inorganic Chemistry, Institute of Chemistry, Faculty of Science, Pavol Jozef Šafárik University in Košice, Moyzesova 11, Košice 040 01, Slovakia  
E-mail: juraj.cernak@upjs.sk

[b] Prof. Dr. L. R. Falvello  
Department of Inorganic Chemistry/INMA, Aragón Nanoscience and Materials Institute, University of Zaragoza, C/Pedro Cerbuna, 12, Zaragoza 50009, Spain

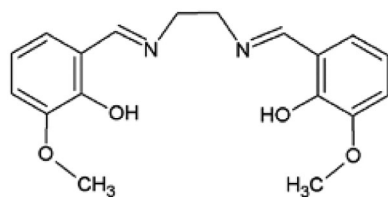
[c] Dr. M. Tomás, Prof. Dr. I. Ara  
Department of Inorganic Chemistry/ISQCH, Chemical Synthesis and Homogeneous Catalysis Institute, University of Zaragoza, C/Pedro Cerbuna 12, Zaragoza 50009, Spain  
E-mail: irene.ara@unizar.es

[d] Prof. Dr. J. Titiš  
Department of Chemistry, Faculty of Natural Sciences, University of SS. Cyril and Methodius, Nám J. Herdu 2, Trnava 917 01, Slovakia

[e] Prof. Dr. R. Boča  
Faculty of Health Science, University of SS. Cyril and Methodius, Nám J. Herdu 2, Trnava 917 01, Slovakia

Supporting information for this article is available on the WWW under <https://doi.org/10.1002/chem.202500376>

© 2025 The Author(s). Chemistry – A European Journal published by Wiley-VCH GmbH. This is an open access article under the terms of the Creative Commons Attribution-NonCommercial-NoDerivs License, which permits use and distribution in any medium, provided the original work is properly cited, the use is non-commercial and no modifications or adaptations are made.



Scheme 1. The schematic structure of Schiff-base  $H_2(o\text{-van-en})$ .

nitroxyl radical 4,4-dimethyl-2,2-bis(pyridin-2-yl)-1,3-oxazolidine-3-oxyl) slow magnetic relaxation was observed below 20 K.<sup>[10]</sup> A search in the CSD<sup>[11]</sup> reveals that only 5 Eu(III) complexes based on a heterobimetallic  $\{\text{Tr}(o\text{-van-en})\text{Eu}\}$  structural unit (Tr is any 3d metal including zinc)<sup>[12–16]</sup> were structurally characterized; these were mainly studied due to their catalytic activity or luminescence.<sup>[12–16]</sup> The sole magnetically characterized complex was  $[\text{Zn}_2\text{Eu}_3(o\text{-van-en})_3(\text{N}_3)_5(\text{OH})_2]$ , but this complex did not display slow magnetic relaxation.<sup>[15]</sup>

The same type of Sm(III) complexes based on a  $\{\text{Tr}(o\text{-van-en})\text{Sm}\}$  structural unit were also scarcely studied. The search in Cambridge Structural Database<sup>[11]</sup> returned only 6 such Sm(III) complexes.<sup>[5,17–21]</sup> Among these, 4 complexes, namely  $\{[(\text{CH}_3\text{OH})\text{Cu}(o\text{-van-en})_2\text{Sm}(\text{NO}_3)] [\text{Ni}(\text{mnt})_2] (\text{mnt} = \text{maleonitriledithiolato})\}^{[18]}$   $\{[\text{Cu}_2(o\text{-van-en})_2 \text{Sm}(\text{H}_2\text{O})] \{\text{W}(\text{CN})_8\}_n \cdot 3\text{nH}_2\text{O}\}^{[19]}$   $[\text{Sm}(\text{NO}_3)\{\text{Zn}(o\text{-van-en}) (\text{SCN})\}_2]^{[20]}$  and  $\{[\text{Cu}(o\text{-van-en})\text{Sm}(\text{H}_2\text{O})_4] [\text{Cr}(\text{CN})_6] \cdot \text{CH}_3\text{OH} \cdot 3\text{H}_2\text{O}\}_n^{[21]}$  were magnetically studied but AC components of these complexes were silent. We note that in all these Eu(III) and Sm(III) complexes the most popular coligands are nitrate ligands and in no case are halogenido coligands found.

We primarily focused on replacing diamagnetic square coordinated Ni(II) with paramagnetic Cu(II) and monitoring the influence of this change on the crystal and supramolecular structures. We have used the Schiff base  $H_2L$  ( $H_2L = H_2(o\text{-van-en}) = N,N'$ -ethylene-bis(3-methoxysalicylaldehyde)) (Scheme 1) and by combination of chlorides of Eu(III), Sm(III), and Gd(III) we prepared, characterized, and conducted magnetic studies on a family of isostructural dinuclear complexes:  $[\text{CuCl}(o\text{-van-en})\text{Ln}(\text{H}_2\text{O})_3\text{Cl}]\text{Cl} \cdot \text{EtOH}$  (Ln = Sm (1), Eu (2), Gd (3)) – that is, with the 4f element Gd and with the two elements preceding it in the lanthanoid series. The previously mentioned Tb compound<sup>[7]</sup> is essentially isostructural with compounds 1–3 with MeOH substituting EtOH; its AC susceptibility measurements did not show slow relaxation of magnetization. Recently, analogous Cu/4f heterobimetallic complexes (Ln = Ce, Gd, Tb, Dy, Er, Yb), but with  $\text{NO}_3^-$  instead of  $\text{Cl}^-$ , were studied; these were based on a bicompartamental ligand formed by condensation of ethylenediamine and 2,3-dihydroxybenzaldehyde; all of these nitrate complexes displayed AC responses.<sup>[22]</sup>

## 2. Results and Discussion

### 2.1. Syntheses and Identification

The ligand  $H_2(o\text{-van-en})$  was prepared under mild conditions without necessity of refluxing and, after its isolation was used for

preparation of the metalloligand  $[\text{Cu}(o\text{-van-en})]$ . The isostructural dinuclear complexes  $[\text{CuCl}(o\text{-van-en})\text{Ln}(\text{H}_2\text{O})_3\text{Cl}]\text{Cl} \cdot \text{C}_2\text{H}_6\text{O}$  (Ln = Sm (1), Eu (2), Gd (3)) in single crystal form were prepared by the horizontal diffusion technique<sup>[23]</sup> by reacting  $[\text{Cu}(o\text{-van-en})\text{H}_2\text{O}]$  with  $\text{SmCl}_3 \cdot 6\text{H}_2\text{O}$ ,  $\text{EuCl}_3 \cdot 6\text{H}_2\text{O}$ , and  $\text{GdCl}_3 \cdot 6\text{H}_2\text{O}$ , respectively. The prepared complexes are new but the analogous complex  $[\text{Cu}(o\text{-van-en})\text{ClTb}(\text{H}_2\text{O})_3\text{Cl}]\text{Cl} \cdot \text{CH}_3\text{OH}$  with a methanol solvate molecule prepared by a different method was recently reported.<sup>[7]</sup> The isolated solid complexes were characterized by CHN analyses and IR spectroscopy. The most characteristic absorption band is due to stretching vibration of the imine bond: this was found at  $1637 \text{ cm}^{-1}$  (Figure S1).

Due to the presence of the solvate ethanol molecule the thermal curves of 1 were taken (Figure S2). The complex 1 is stable up to 60 °C when desolvation starts. The weight loss up to 95 °C is 11.5% which corresponds to the loss of the ethanol solvate molecule and two aqua ligands from the formula unit (calculated weight loss is 11.0%). Further heating leads to decomposition of the organic part of the sample. The weight of the final solid residue at 500 °C is 32.7% which indicates formation of the expected mixture of CuO and SmOCl (calc. 31.9%). For all three complexes the powder diffractograms of the bulk samples were taken (Figures S3–S5). Comparison with the simulated ones corroborated their phase purity and phase identity with the single-crystal structures (see below).

### 2.2. Crystal Structures

The three crystal structures 1–3 are isostructural so we will limit our description and discussion to complex 1 with the corresponding geometric parameters of 2 and 3 given in parentheses. All three crystal structures were studied at 100 K (Table S1).

The ionic crystal structure of  $[\text{CuCl}(o\text{-van-en})\text{SmCl}(\text{H}_2\text{O})_3]\text{Cl} \cdot \text{C}_2\text{H}_6\text{O}$  (1) consists of the dinuclear complex cation  $[\text{CuCl}(o\text{-van-en})\text{SmCl}(\text{H}_2\text{O})_3]^+$ , a chloride counterion and a solvate ethanol molecule (Figure 1). In the isostructural complexes 2 and 3 the Sm(III) atoms are replaced by Eu(III) and Gd(III) atoms (Figure S6). The two central atoms, Cu(II) and Sm(III), occupy the smaller and larger cavities in the bicompartamental Schiff base ligand, respectively. The two central atoms are bridged by a pair of oxygen atoms from the Schiff base which leads to their proximity, with a  $\text{Cu} \cdots \text{Sm}$  distance of  $3.4450(2) \text{ \AA}$  ( $3.4335(4) \text{ \AA}$  for Eu and  $3.4367(5) \text{ \AA}$  for Gd).

A search in CSD<sup>[11]</sup> has revealed that up to now were structurally characterized 16 analogous complexes based on the structural unit  $\{\text{Cu}(o\text{-van-en})\text{Ln}\}$ , these are gathered in Table S2 in the Supplementary file. In almost all these complexes the coligands bound to the Ln(III) atoms are O-donor ligands, mainly nitrate ones. The sole exception is the  $[\text{CuCl}(o\text{-van-en})\text{Tb}(\text{H}_2\text{O})_3\text{Cl}]\text{Cl} \cdot \text{CH}_3\text{OH}$  complex.<sup>[7]</sup> So the studied complexes 1–3 with  $\text{ClO}_7^-$  donor set and with central atoms Sm(III), Eu(III), and Gd(III), resp., can be considered as new ones in the class of Cu(II)/Ln(III) heterobimetallic complexes with a  $\{\text{Cu}(o\text{-van-en})\text{Ln}\}$  structural unit.

We note that the preference of Ln(III) central atoms to be coordinated by hard O-donor ligands is well-known and can be

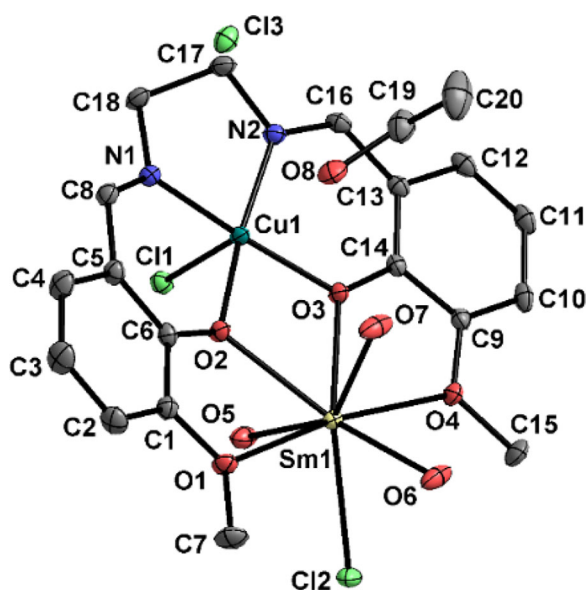


Figure 1. Molecular structure of  $[\text{CuCl}(\text{o-van-en})\text{SmCl}(\text{H}_2\text{O})_3] \cdot 2\text{H}_2\text{O}$  (1).

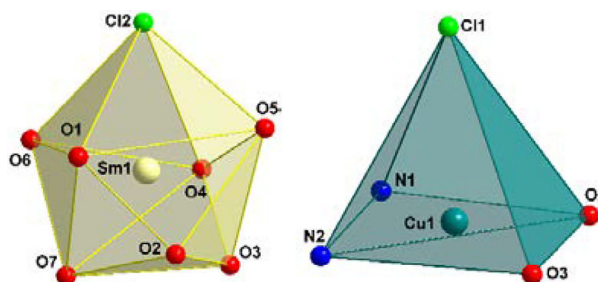


Figure 2. Coordination polyhedra around the Sm(III) (left) and Cu(II) central atoms (right) in 1.

documented by ratio 24697/346 where the numbers mean the returned hits in CSD<sup>[11]</sup> for queries formed by respective coordination polyhedra  $\{\text{LnO}_8\}$  and  $\{\text{LnClO}_7\}$  where Ln is any lanthanide atom. It is expected that inclusion of the chlorido ligand in the coordination sphere of the Ln(III) atom may enhance the anisotropy of its coordination sphere.

The distance of Sm1–Cl2 is 2.7024(5) Å, which is in line with the corresponding value Sm1–Cl1 = 2.682(2) Å reported for  $[\text{Sm}(\text{3,5-Bu}^t\text{-2-O-C}_6\text{H}_4\text{CH} = \text{N-8-C}_9\text{H}_6\text{N})(\text{CH}_3\text{C}_5\text{H}_4\text{Cl})(\text{THF})] \cdot \text{THF}$ .<sup>[24]</sup> The distances of Sm(III) to O5, O6, and O7 (aqua ligands) in 1 are in the range 2.4175(14)–2.4239(14) Å. Similar Sm–O bond distances of 2.503(3) and 2.466(3) Å were found in the nitrate complex  $[\text{Cu}(\text{o-van-en})\text{Sm}(\text{NO}_3)_2(\text{H}_2\text{O})_2](\text{NO}_3)$ .<sup>[5]</sup>

The coordination polyhedra of the Sm(III) and Cu(II) central atoms are displayed on Figure 2. The polyhedra in analogous complexes 2 and 3 are shown in the Supporting Information file (Figures S7 and S8). As follows from the calculations using the SHAPE program<sup>[25]</sup> the coordination polyhedron around the Sm(III) atom has an intermediate shape between triangular dodecahedron and biaugmented trigonal prism (Table S2). The coordination polyhedron around the Cu(II) atom can be viewed as spherical square pyramid (Table S2). The distances between Cu(II) and the plane formed by N1, N2, O2, and O3 atoms from

Cu1–N1	1.9180(16)	N1–Cu1–N2	86.27(7)
Cu1–O2	1.9243(13)	N1–Cu1–O2	94.51(6)
Cu1–O3	1.9250(13)	N1–Cu1–O3	170.67(6)
Cu1–Cl1	2.7518(5)	N1–Cu1–Cl1	96.89(5)
Sm1–O1	2.5625(13)	N2–Cu1–O2	169.04(6)
Sm1–O2	2.3806(12)	N2–Cu1–O3	94.83(6)
Sm1–O3	2.3590(12)	N2–Cu1–Cl1	91.96(5)
Sm1–O4	2.5646(13)	O2–Cu1–O3	82.67(5)
Sm1–O5	2.4239(14)	O2–Sm1–O3	64.87(4)
Sm1–O6	2.4175(14)	O2–Cu1–Cl1	98.79(4)
Sm1–O7	2.4192(14)	O3–Cu1–Cl1	92.33(4)
Sm1–Cl2	2.7024(5)	O1–Sm1–O2	61.85(4)
O1–Sm1–O3	126.52(4)	O1–Sm1–O5	94.73(5)
O1–Sm1–O6	87.89(5)	O1–Sm1–O7	84.04(5)
O1–Sm1–Cl2	88.28(3)	O1–Sm1–O4	171.44(4)
O2–Sm1–O5	75.35(5)	O2–Sm1–O6	132.35(5)
O2–Sm1–O7	73.39(5)	O3–Sm1–O5	75.92(5)
O3–Sm1–O6	127.04(5)	O3–Sm1–O7	76.96(5)
O3–Sm1–Cl2	135.73(3)	O5–Sm1–O6	147.69(5)
O5–Sm1–O7	145.07(5)	O5–Sm1–Cl2	74.57(3)
O6–Sm1–O7	67.26(5)	O6–Sm1–Cl2	73.32(4)
O7–Sm1–Cl2	140.02(4)	O3–Sm1–O4	61.90(4)

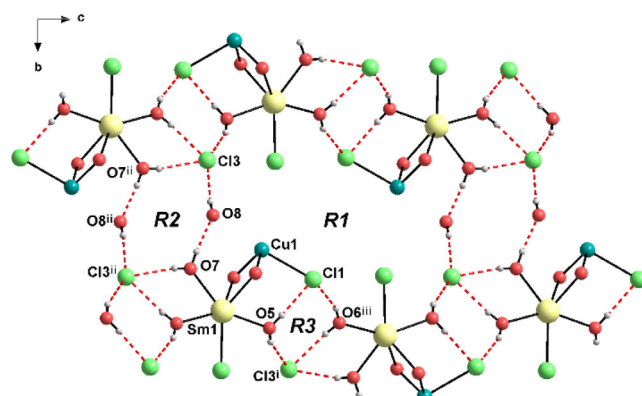


Figure 3. Supramolecular structure of 1 with hydrogen bonds (red dashed lines). Symmetry codes: i:  $-x+1/2, y+1/2, -z+3/2$ ; ii:  $-x+1, -y+1, -z+1$ ; iii:  $x+1/2, -y+3/2, z-1/2$ .

the  $(\text{o-van-en})^{2-}$  ligand are 0.1668(3) Å in 1, 0.1722(3) Å in 2, and 0.1747(4) Å in 3). Selected geometric parameters in 1 are displayed in Table 1 while those for 2 and 3 are gathered in Tables S4 and S5. A comparison of the respective Ln–O and Ln–Cl distances is given in Table S6.

The supramolecular structure of 1 (as well as of 2 and 3) is governed by hydrogen bonds of the O–H...Cl and O–H...O types (Figure 3, Figure S9, Table 2, and Figures S10 and S11; Tables S7 and S8 for 2 and 3). O–H...Cl hydrogen bonds with participation of the Cl1 chlorido ligand and the Cl3 chloride anion link the individual dinuclear molecules yielding a supramolecular chain running along the *c*-axis; within these chains the

Table 2. Possible hydrogen bonds in 1.				
D—H...A	D—H [Å]	H...A [Å]	D...A [Å]	D—H...A [°]
O8—H81...Cl3	0.80(3)	2.33(3)	3.1288(16)	173(3)
O5—H105...Cl1	0.84(1)	2.22(1)	3.0591(15)	177(3)
O5—H205...Cl3 <sup>i</sup>	0.83(1)	2.474(15)	3.2428(15)	154(2)
O6—H106...Cl3 <sup>ii</sup>	0.84(1)	2.298(11)	3.1300(15)	173(3)
O6—H206...Cl1 <sup>iii</sup>	0.83(1)	2.351(16)	3.1211(15)	154(3)
O7—H107...O8	0.84(1)	1.828(11)	2.654(2)	168(3)
O7—H207...Cl3 <sup>ii</sup>	0.83(1)	2.344(11)	3.1645(15)	169(3)

Symmetry operations: i:  $-x+1/2, y+1/2, -z+3/2$ ; ii:  $-x+1, -y+1, -z+1$ ; iii:  $x+1/2, -y+3/2, z-1/2$ .

individual Sm(III) atoms are at a distance of 8.8841(5) Å (Sm1 and Sm1<sup>iii</sup>; iii:  $x+1/2, -y+3/2, z-1/2$ ). These supramolecular chains are interconnected along the *b*-axis by additional O—H...O and O—H...Cl hydrogen bonds in which are involved the OH group of the ethanol solvate molecule (O8), the O7 aqua ligand and the chloride anion Cl3. As a result, a 2D supramolecular structure is formed. The shortest distance between Sm(III) atoms along the *b*-axis is 11.1062(7) Å (Sm1 and Sm1<sup>i</sup>; i:  $-x+1/2, y+1/2, -z+3/2$ ).

### 2.3. DC Magnetic Data

DC magnetic susceptibility was taken between  $T = 1.9 - 300$  K at  $B = 0.1$  T and magnetization data up to  $B = 7$  T at  $T = 2.0$  and  $5.0$  K (Figure 4).

The molar magnetic susceptibility for complex 1 increases monotonically as the temperature decreases, up to approximately  $T = 5$  K. Below this temperature, it increases more sharply with a further decrease in temperature. The effective magnetic moment takes a value of  $2.50 \mu_B$  at  $T = 300$  K and gradually decreases to  $1.85 \mu_B$  at  $T = 25$  K upon cooling. The room temperature  $\mu_{\text{eff}}$  value corresponds to a single Sm(III) ion (for the ground term  $^6H_{5/2}$   $\mu_{\text{eff}} = 0.83 \mu_B$ ) interacting with a spin  $S = 1/2$  system ( $\mu_{\text{eff}} = 1.73 \mu_B$  for  $g = 2$ ). With a further decrease in temperature,  $\mu_{\text{eff}}$  drops sharply to  $0.86 \mu_B$  at  $T = 1.9$  K probably owing to the antiferromagnetic coupling between Cu(II) and Sm(III). The magnetization per formula unit,  $M_1 = M_{\text{mol}}/N_A \mu_B$ , adopts a subnormal value of  $M_1 = 0.41$  at  $T = 2.0$  K and  $B = 5.0$  T, which is lower than the expected value of  $M_1 = 1$  for  $S = 1/2$ , and deviates from the predicted Brillouin function behaviour. For complex 2  $\mu_{\text{eff}} = 3.93 \mu_B$  at  $T = 300$  K and gradually decreases with temperature up to a value of  $2.11 \mu_B$  at  $T = 1.9$  K. For the Eu(III) ion, the ground electronic term  $^7F_0$  is nonmagnetic. However, at higher temperatures, thermal population of the first excited state,  $^7F_1$ , occurs, leading to an increase in the effective magnetic moment at room temperature. The molar magnetization adopts a value of  $M_1 = 1.34 N_A \mu_B$  at  $T = 2.0$  K and  $B = 5.0$  T indicating a saturation effect. Complex 3 contains Gd(III) ion for which the ground atomic term is  $^8S_{7/2}$  ( $L = 0$ ). At room temperature  $\mu_{\text{eff}} = 8.11 \mu_B$ . This value remains constant during cooling up to  $T = 120$  K, subsequently it increases slightly, reaching the value  $9.10 \mu_B$  at  $T = 1.9$  K. Thus, a weak ferromagnetic interaction between the Gd(III) and Cu(II)

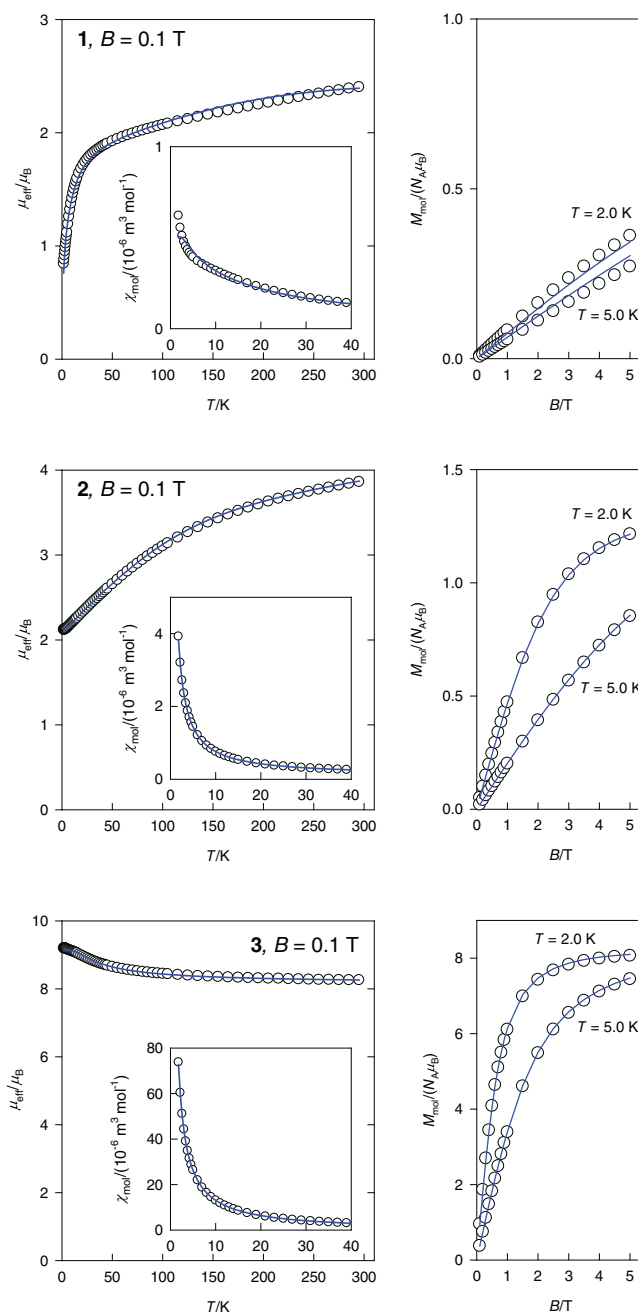


Figure 4. DC susceptibility data for 1–3. Lines — calculated by a simultaneous fitting the susceptibility and magnetization data.

spins can be assumed. The magnetization in this case reaches full saturation ( $M_1 = 8.0 N_A \mu_B$ ) already at  $B = 5.0$  T.

Experimental magnetic data of complexes 1 and 2 have been fitted using the following model Hamiltonian

$$\hat{H}_1 = \lambda \left( \vec{L}_{Ln} \cdot \vec{S}_{Ln} \right) - J_{\text{ex}} \left( \vec{S}_{Cu} \cdot \vec{S}_{Ln} \right) + \Delta_{\text{ax}} \left( \hat{L}_{Ln,z}^2 - \frac{\hat{L}_{Ln}^2}{3} \right) + \mu_B B \left( g_{L,Ln} \vec{L}_{Ln} + g_{S,Ln} \vec{S}_{Ln} + g_{S,Cu} \vec{S}_{Cu} \right) \quad (1)$$

where  $L_n = \text{Sm}$  for 1 and  $\text{Eu}$  for 2. The individual terms in the above Hamiltonian describe: spin-orbit coupling, isotropic

Complex	$\lambda(\text{Ln})$ [cm <sup>-1</sup> ]	$J(\text{Ln}-\text{Cu})$ /[cm <sup>-1</sup> ]	$\Delta_{\text{ax}}$ [cm <sup>-1</sup> ]	$g_{\text{S,Cu}}$	$R(\chi)$ [%]	$R(M)$ [%]
1 [a]	275	-13.4	12.0	2.21	7.6	9.0
2 [a]	300	1.2	12.0	2.38	1.7	0.5
3 [a,b]		8.2		2.33	1.2	0.5

[a]  $g_{\text{L,Ln}} = 1$ ,  $g_{\text{S,Ln}} = 2$ , fixed.  
[b]  $\chi_{\text{TIM}} = -1.9 \times 10^{-9} \text{ m}^3 \text{ mol}^{-1}$  (temperature independent magnetism).

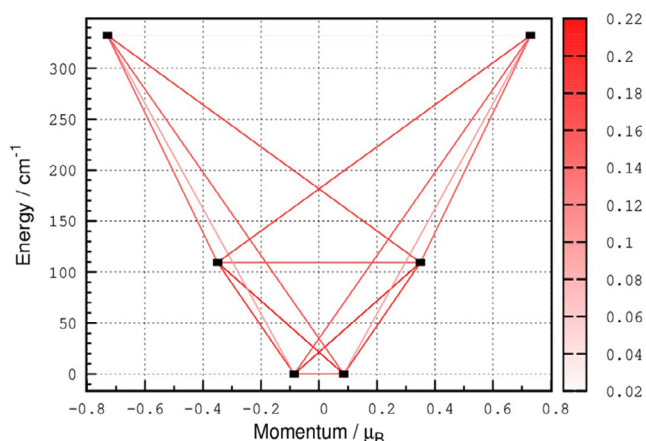


Figure 5. Magnetization blocking barrier for complex 1 (Sm(III)–Zn(II)) calculated using single\_aniso module (CASSCF-NEVPT2). The side bar represents values of the corresponding matrix elements of the transversal magnetic moment.

exchange interaction, axial crystal field effect, and Zeeman interaction. In the case of complex 3, the Hamiltonian used was in the following form

$$\hat{H}_2 = -J_{\text{ex}} (\vec{S}_{\text{Cu}} \cdot \vec{S}_{\text{Gd}}) + \mu_{\text{B}} B (g_{\text{S,Gd}} \vec{S}_{\text{Gd}} + g_{\text{S,Cu}} \vec{S}_{\text{Cu}}) \quad (2)$$

The obtained optimal parameters are summarized in Table 3. A weak antiferromagnetic exchange interaction was confirmed in the case of complex 1. On the contrary, in complexes 2 and 3, a ferromagnetic type interaction is observed.

A DFT calculation was performed for complex 3. Gd(III) is single reference system (4f<sup>7</sup> configuration), so DFT methods are fully applicable in this case (unlike Sm(III) and Eu(III)). This calculation clearly confirmed the ferromagnetic interaction between the Gd(III) and Cu(II) ions ( $J_{\text{Gd}-\text{Cu}}^{\text{B3LYP}} = +4.55 \text{ cm}^{-1}$ ). *Ab initio* calculations were performed for complex 1, which allowed a detailed view of the mechanism of magnetic relaxation of the Sm(III) ion within the ground term <sup>6</sup>H<sub>5/2</sub>. This term split into three Kramers doublets (KDs) span an energy window of 332 cm<sup>-1</sup>. The main components of the *g*-tensor of the ground KD have the values  $g_{\text{xx}} = 0.736$ ,  $g_{\text{yy}} = 0.470$ , and  $g_{\text{zz}} = 0.170$ . Wave function analysis suggests that the ground KD has predominantly  $|\pm 1/2\rangle$  character. The first excited KD  $|\pm 3/2\rangle$  is located 109 cm<sup>-1</sup> above the ground one. Magnetization blocking barrier calculated for Sm(III)–Zn(II) shows that in this system fast relaxation already applies within the ground multiplet (Figure 5).

## 2.4. AC Magnetic Data

AC magnetic susceptibility has been taken with the MPMS3 magnetometer (Quantum Design) in several regimes at  $B_{\text{AC}} = 0.3 \text{ mT}$ , using various  $B_{\text{DC}}$  field, frequency  $f = 0.1 - 1000 \text{ Hz}$ , and temperature  $T = 1.9 - 4.5 \text{ K}$ . For complex 1, AC measurements did not confirm slow magnetic relaxation, which corresponds to the *ab initio* prediction. This observation is in line with the review paper on heteronuclear Sm(III)/3d metal complexes with salen type ligands: several Sm(III) complexes were magnetically characterized but none displayed SMM behaviour.<sup>[26]</sup> To our best knowledge, the first Sm(III) complex ([SmL<sub>2</sub>(DMF)Cl<sub>2</sub>]Cl, L = bis(diphenylphosphino)methane-dioxide) with slow magnetic relaxation was reported only in 2020.<sup>[27]</sup>

The AC susceptibility data for 3 are reviewed in Figures 6–8. The first scan refers to the varied external field at  $T = 2.0 \text{ K}$  for a set of trial frequencies (Figure 6). It is seen that the out-of-phase component passes through a maximum at ca  $B_{\text{DC}} \sim 0.3 \text{ T}$  and much larger amplitude show the low-frequency data ( $f = 1.1 \text{ Hz}$ ). It is proven that the complex [Gd–Cu] exhibits a slow magnetic relaxation that depends on the external DC magnetic field and frequency of the AC field. A nonzero  $\chi''$  component at  $B_{\text{DC}} = 0$  indicates that the complex is a nano magnet.

A dense mapping of the  $\chi_{\text{AC}}(f, T)$  functions at  $B_{\text{DC}} = 0.3 \text{ T}$  is presented in Figure 7. It is seen that the frequency dependence of the out-of-phase component exhibits two peaks which confirm two-mode relaxation processes. The low-frequency (LF) mode dominates at low temperature and the peak value at  $f_{\text{max}} = 0.4 \text{ Hz}$  indicates the low-frequency relaxation time  $\tau_{\text{LF}} = 1/(2\pi f_{\text{max}}) = 0.4 \text{ s}$ . The data fitting with the two-set Debye model confirms this estimate (Table S9). On heating the LF mode is attenuated in favour of the high-frequency (HF) mode.

The AC susceptibility data for 2 are reviewed in Figures 9–11. The AC response is very weak, as the Cu(II) centre contributes with the spin  $s = 1/2$  and the Eu(III) centre has the ground state nonmagnetic, <sup>7</sup>F<sub>0</sub>. Also this system shows a field supported slow magnetic relaxation with a single relaxation mode. The relaxation time at  $B_{\text{DC}} = 0.3 \text{ T}$  and  $T = 1.9 \text{ K}$  is  $\tau = 64 \text{ ms}$  (Table S10).

Magnetic studies on Eu(III) complexes are rather scarce.<sup>[28–30]</sup> The Eu(III)–Cu(II) diad shows a field induced slow magnetic relaxation with two relaxation channels; the relaxation time is  $\tau_{\text{LF}} (1.9 \text{ K}, 0.4 \text{ T}) = 25 \text{ ms}$  for the low-frequency relaxation channel.<sup>[14]</sup>

## 3. Conclusion

Three new heterobimetallic complexes [CuCl(*o-van-en*)LnCl(H<sub>2</sub>O)<sub>3</sub>]Cl·C<sub>2</sub>H<sub>6</sub>O (Ln = Sm (1), Eu (2), Gd (3)) based on Schiff base type bicompartamental ligand (*o-van-en*)<sup>2-</sup> and with chlorido coligand were prepared and characterized. Isostructural complexes 1, 2, and 3 exhibit ionic crystal structures with dinuclear Cu/Ln complex cations. Within the cations, Cu(II) and Ln(III) central atoms occupy the smaller and larger cavities in the ligand, respectively, and they are linked by a pair of monoatomic O-bridges. Ethanol solvate molecules complete the final compositions of 1–3. The Cu(II) atoms in 1–3 exhibit square pyramidal

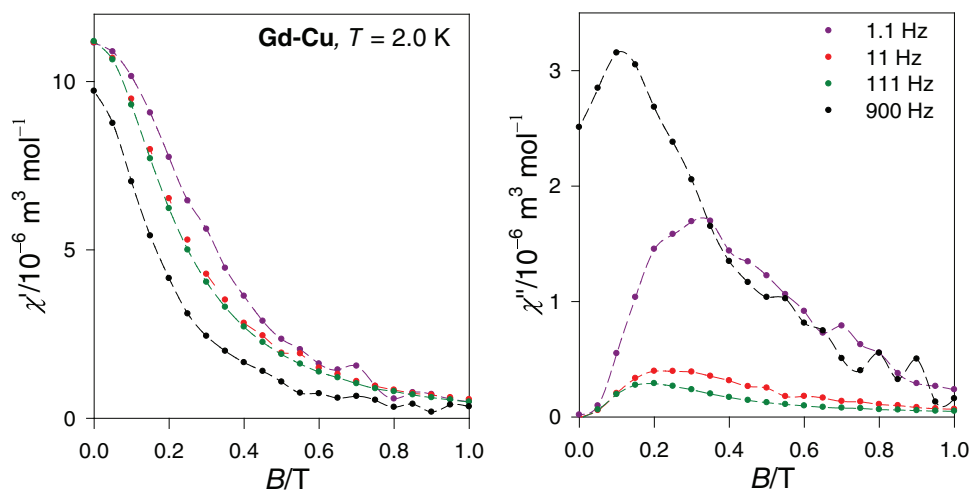


Figure 6. AC susceptibility data for Gd-Cu complex at  $T = 2.0$  K.

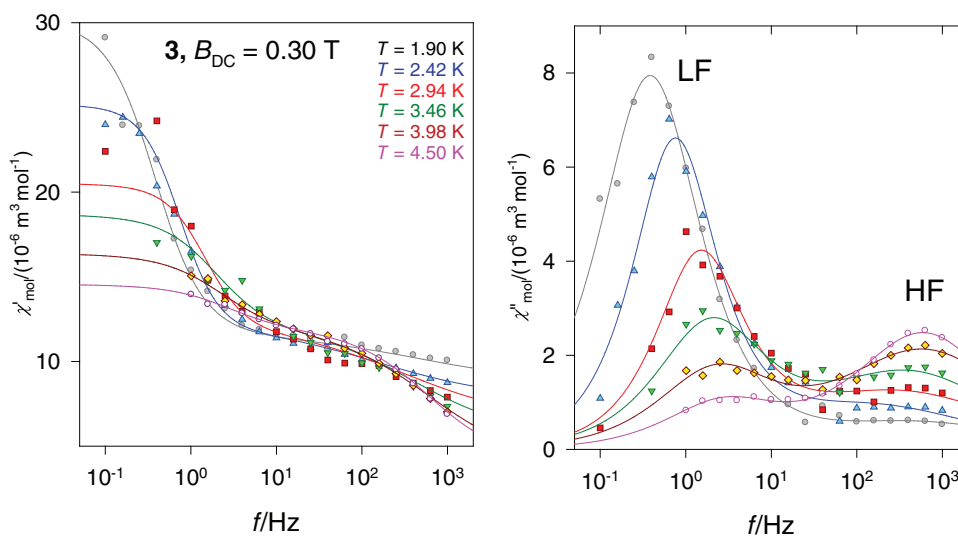


Figure 7. AC susceptibility data for Gd-Cu complex 3 at  $B_{DC} = 0.3$  T.

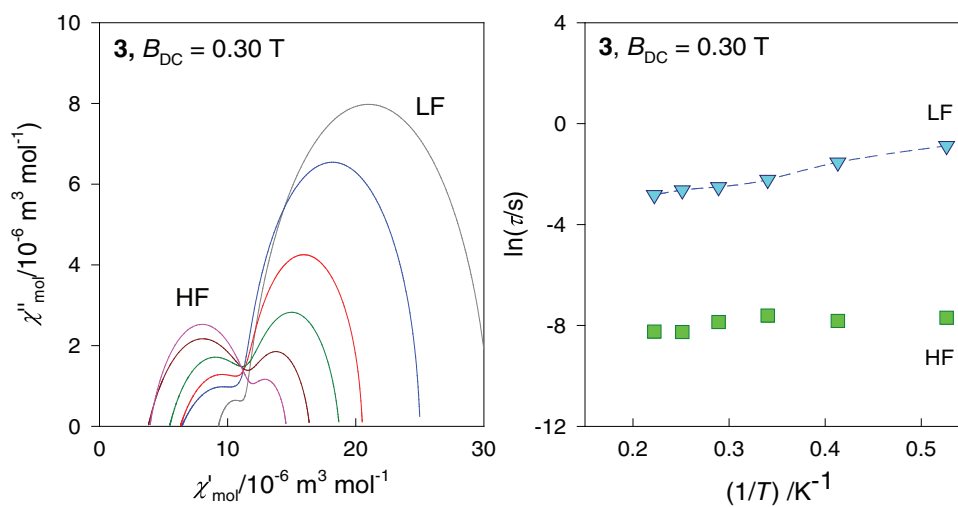


Figure 8. AC susceptibility functions: Argand plot (left) and temperature evolution of relaxation time for 3.

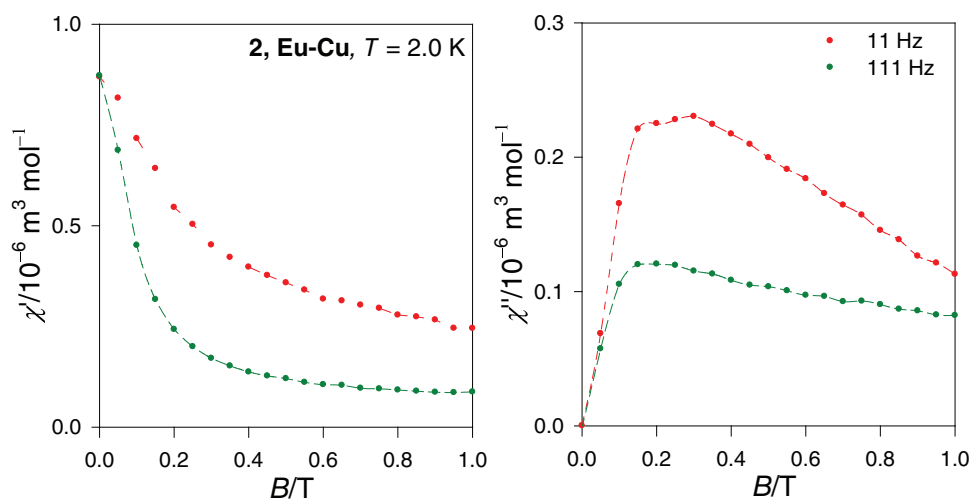


Figure 9. AC susceptibility data for Eu–Cu complex 2 at  $T = 2.0$  K.

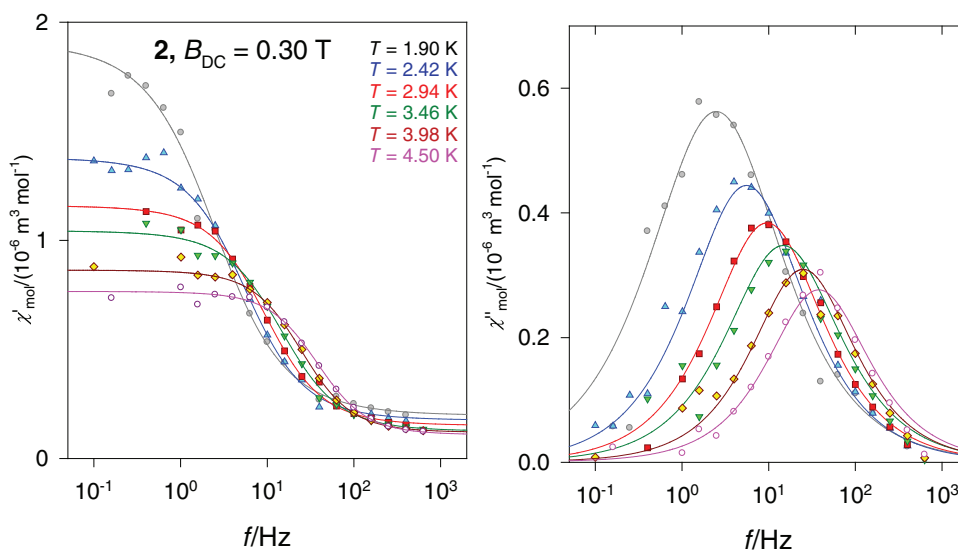


Figure 10. AC susceptibility data for Eu–Cu complex 2 at  $B_{DC} = 0.3$  T.

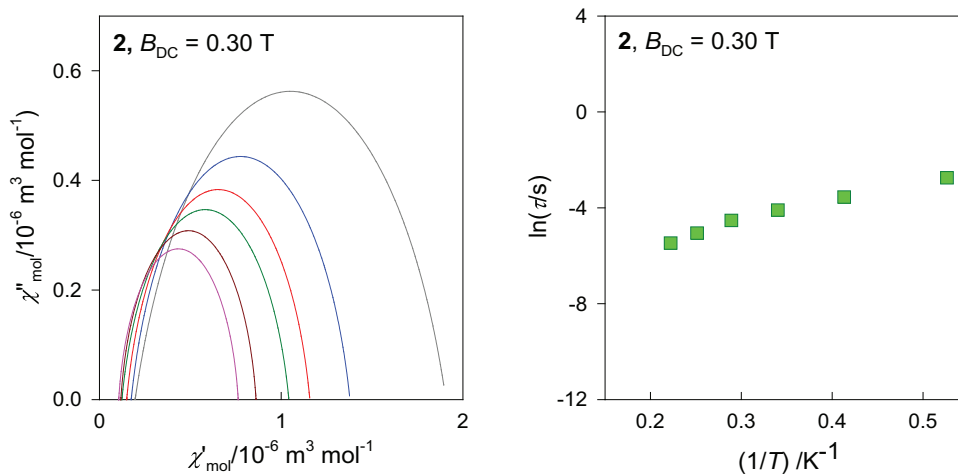


Figure 11. AC susceptibility functions: Argand plot (left) and temperature evolution of relaxation time for 2.

coordination ( $\tau = 0.026$  (1), 0.024 (2), and 0.025 (3)) with the chlorido ligand placed in the apical position. The coordination numbers of the Ln(III) atoms are eight with the chromophore  $\{\text{LnO}_7\text{Cl}\}$  and their shape is close to a triangular dodecahedron. The 2D supramolecular structures of **1**, **2**, and **3** are built up of O—H...Cl and O—H...O types of hydrogen bonds. The magnetic properties reveal that the complexes **2** and **3** exhibit the field supported slow magnetic relaxation; the relaxation time at  $T = 1.9$  K and  $B_{DC} = 0.3$  T is  $\tau = 64$  ms and  $\tau_{LF} = 413$  ms for **2** and **3**, respectively.

## Supporting Information

Deposition Numbers [2375691](#) (1), [2375692](#) (2), and [2375693](#) (3) contain the supplementary crystallographic data for this paper. These data are provided free of charge by the joint Cambridge Crystallographic Data Centre and Fachinformationszentrum Karlsruhe Access Structures service <http://www.ccdc.cam.ac.uk/structures>. The authors have cited additional references within the Supporting Information.<sup>[31–52]</sup>

## Acknowledgements

Funded by the EU NextGenerationEU through the Recovery and Resilience Plan for Slovakia under the project No. 09103-03-V05-00008. Slovak grant agency VEGA 1/0191/22 is acknowledged for financial support. Funding was also provided by Spanish Ministerio de Ciencia, Innovación y Universidades (Grant PID2021-124880NB-I00), the European Union Regional Development Fund (FEDER), and the Diputación General de Aragón (Project M4, E11\_23R).

## Conflict of Interests

The authors declare no conflict of interest.

## Data Availability Statement

The data that support the findings of this study are available in the supplementary material of this article.

**Keywords:** chlorido ligand · Cu(II)-Ln(III) dinuclear complex · schiff base · slow magnetic relaxation · x-ray structure

- [1] M. A. Halcrow (ed.), *Spin-crossover materials: properties and applications*. John Wiley & Sons, 2013. Online ISBN: 9781118519301
- [2] S. G. McAdams, A. M. Ariciu, A. K. Kostopoulos, J. P. S. Walsh, F. Tuna, *Coord. Chem. Rev.* **2017**, *346*, 216.
- [3] A. Bencini, C. Benelli, A. Caneschi, R. L. Carlin, A. Dei, D. Gatteschi, *J. Am. Chem. Soc.* **1985**, *107*, 8128.
- [4] S. A. Cotton, P. R. Raithby, *Coord. Chem. Rev.* **2017**, *340*, 220.
- [5] Y. Sui, X. N. Fang, Y. A. Xiao, Q. Y. Luo, M. H. Li, *Acta Cryst.* **2006**, *E62*, m2230.
- [6] K. Wang, J. Zhang, J. Lu, P. Jing, L. Li, *Inorg. Chim. Acta* **2019**, *490*, 51.

- [7] X. Feng, W. Zhou, Y. Li, H. Ke, J. Tang, R. Clérac, Y. Wang, Z. Su, E. Wang, *Inorg. Chem.* **2012**, *51*, 2722.
- [8] A. Vráblová, M. Tomás, L. R. Falvello, L. Dlháň, J. Titiš, J. Černák, R. Boča, *Dalton Trans.* **2019**, *48*, 13943.
- [9] P. Bhunia, S. Maity, T. K. Ghosh, A. Mondal, J. Mayans, A. Ghosh, *Dalton Trans.* **2024**, *53*, 9171.
- [10] L. Sorace, A. A. Dmitriev, M. Perfetti, K. E. Vostrikova, *Chem. Sci.* **2025**, *16*, 218.
- [11] C. R. Groom, I. J. Bruno, M. P. Lightfoot, S. C. Ward, *Acta Cryst.* **2016**, *B72*, 171.
- [12] O. V. Amirkhanov, O. V. Moroz, K. O. Znovjyak, T. Y. Sliva, L. V. Penkova, T. Yushchenko, L. Szyrwił, I. S. Konovalova, V. V. Dyakonenko, O. V. Shishkin, V. M. Amirkhanov, *Eur. J. Inorg. Chem.* **2014**, *23*, 3720.
- [13] S. Zhao, X. Lü, A. Hou, W.-Y. Wong, W.-K. Wong, X. Yang, R. A. Jones, *Dalton Trans.* **2009**, 9595.
- [14] W.-J. Jin, L.-Q. Ding, Z. Chu, L.-L. Chen, X.-Q. Lü, X.-Y. Zheng, J.-R. Song, D.-D. Fan, *J. Mol. Catal. A Chem.* **2011**, *337*, 25.
- [15] C. E. Burrow, T. J. Burchell, P.-H. Lin, F. Habib, W. Wernsdorfer, R. Clérac, M. Murugesu, *Inorg. Chem.* **2009**, *48*, 8051.
- [16] T. Gao, P.-F. Yan, G.-M. Li, G.-F. Hou, J.-S. Gao, *Inorg. Chim. Acta* **2008**, *361*, 2051.
- [17] G. Xiao, B. Yan, R. Ma, W. J. Jin, X. Q. Lu, L. Q. Ding, C. Zeng, L. L. Chen, F. Bao, *Polym. Chem.* **2011**, *2*, 659.
- [18] A. M. Madalan, N. Avarvari, M. Fourmigué, R. Clérac, L. F. Chibotaru, S. Clima, M. Andruh, *Inorg. Chem.* **2008**, *47*, 940.
- [19] H. Zhou, K. Wu, C. Chen, R. Dong, Y. Liu, X. Shen, *Eur. J. Inorg. Chem.* **2017**, *33*, 3946.
- [20] C. Takehara, P. L. Then, Y. Kataoka, M. Nakano, T. Yamamura, T. Kajiwara, *Dalton Trans.* **2015**, *44*, 18276.
- [21] H. Zhou, C. Chen, K. Wu, Y. Liu, X. Shen, *Eur. J. Inorg. Chem.* **2016**, *30*, 4921.
- [22] E. Costa-Villén, M. Font-Bardia, J. Mayans, A. Escuer, *Cryst. Growth Des.* **2024**, *24*, 5806.
- [23] S. Šterbinská, M. Holub, E. Číž'már, J. Černák, L. R. Falvello, M. Tomás, *Cryst. Growth Des.* **2023**, *23*, 4357.
- [24] L. I. Bangyu, Y. A. O. Yingming, W. A. N. G. Yaorong, Y. Zhang, S. H. E. N. Qi, *J. Rare Earths* **2008**, *26*, 469.
- [25] M. Llunell, D. Casanova, J. Cirera, P. Alemany, S. Alvarez, *SHAPE, version 2.1. Universitat de Barcelona, Spain.* **2013**, 2103.
- [26] P. Middy, A. Konar, S. Chattopadhyay, *J. Mol. Struct.* **2025**, *1333*, 141683.
- [27] Y.-Z. Pan, Q.-Y. Hua, L.-S. Lin, Y.-B. Qiu, J.-L. Liu, A.-J. Zhou, W.-Q. Lin, J.-D. Leng, *Inorg. Chem. Front.* **2020**, *7*, 2335.
- [28] M. Dolai, M. Ali, C. Rajnák, J. Titiš, R. Boča, *New J. Chem.* **2019**, *43*, 12698.
- [29] R. Mičová, Z. Biolková, C. Rajnák, J. Titiš, J. Moncol, A. Bienko, R. Boča, *Dalton Trans.* **2024**, *53*, 1492.
- [30] A. Chakraborty, P. Middy, S. Chattopadhyay, *Inorg. Chim. Acta* **2025**, *581*, 122625.
- [31] A. Elmali, Y. Elerman, *Z. Naturforsch.* **2004**, *B59*, 530.
- [32] S. L. Zhang, X. F. Fan, R. L. Du, B. W. Shen, X. D. Song, X. Q. Wie, S. S. Li, *Polyhedron.* **2021**, *206*, 115336.
- [33] T. Gao, P. F. Yan, G. M. Li, J. W. Zhang, W. B. Sun, M. Suda, Y. Einaga, *Solid State Sci.* **2010**, *12*, 597.
- [34] N. Senyuz, C. Yukseketepe, H. Bati, N. Caliskan, O. Buyukgungor, *J. Chem. Crystallogr.* **2010**, *40*, 989.
- [35] P. F. Yan, Y. Wang, P. Chen, J. W. Zhang, Y. Wang, G. M. Li, *CrystEngComm.* **2010**, *12*, 4084.
- [36] S. L. Zhang, Z. Y. Liu, S. Guo, S. Y. Gu, Y. Shi, S. S. Li, *J. Coord. Chem.* **2021**, 1457.
- [37] S. Zhang, R. Du, X. Fan, X. Zhao, Y. Wang, S. Li, *Crystals* **2023**, *13*, 535, (1–9).
- [38] A. Finelli, A. Crochet, K. M. Fromm, CCDC 1861003: Experimental Crystal Structure Determination, **2024**, <https://doi.org/10.5517/ccdc.csd.cc20gjcd>
- [39] V. Petříček, M. Dušek, L. Palatinus, *Z. Kristallogr. Cryst. Mater.* **2014**, *229*, 345.
- [40] a) A. Le Bail, H. Duroy, J. L. Fourquet, *Mat. Res. Bull.* **1988**, *23*, 447; b) A. Le Bail, *Powder Diffr.* **2005**, *20*, 316.
- [41] Bruker, "Apex3 and SADABS." Bruker AXS Inc., Wisconsin, USA, **2016**.
- [42] L. Krause, R. Herbst-Irmer, G. M. Sheldrick, D. Stalke, *J. Appl. Crystallogr.* **2015**, *48*, 3.
- [43] G. M. Sheldrick, *SHELXL-2018 Program for Crystal Structure Refinement*. University of Göttingen, Göttingen, **2018**.

- [44] L. J. Farrugia, *J. App. Crystallogr.* **2012**, *45*, 849.
- [45] K. Brandenburg, DIAMOND. Crystal Impact GbR, Bonn, Germany, **2008**.
- [46] ChemSketch, version **2012**, *Advanced Chemistry Development, Inc. (ACD/Labs)*, Toronto, Canada.
- [47] F. Neese, *Wiley Interdiscip. Rev.: Comput. Mol. Sci.* **2012**, *2*, 73.
- [48] F. Neese, F. Wennmohs, U. Becker, C. Riplinger, *J. Chem. Phys.* **2020**, *152*, 224108.
- [49] M. Reiher, *Theor. Chem. Accounts* **2006**, *116*, 241.
- [50] D. A. Pantazis, F. Neese, *J. Chem. Theory Comput.* **2009**, *5*, 2229.
- [51] F. Neese, *J. Chem. Physics.* **2005**, *122*, 034107.
- [52] R. Maurice, R. Bastardis, C. D. Graaf, N. Suaud, T. Mallah, N. Guihery, *J. Chem. Theory Comput.* **2009**, *5*, 2977.

---

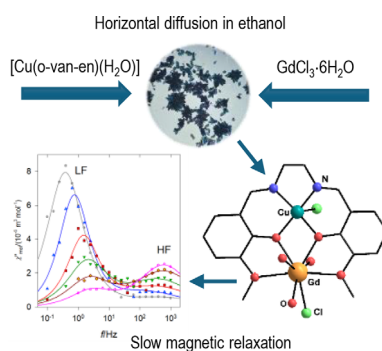
Manuscript received: January 29, 2025

Revised manuscript received: April 17, 2025

Version of record online: ■ ■ ■

## RESEARCH ARTICLE

Three new heterobimetallic complexes  $[\text{CuCl}(\text{o-van-en})\text{LnCl}(\text{H}_2\text{O})_3]\text{Cl}\cdot\text{C}_2\text{H}_6\text{O}$  ( $\text{Ln} = \text{Sm}$  (1),  $\text{Eu}$  (2),  $\text{Gd}$  (3)), with the bicompartamental Schiff-base ligand  $(\text{o-van-en})^{2-}$ , were synthesized using horizontal diffusion. Complexes 2 and 3 exhibit field-supported slow magnetic relaxation, while complex 1 does not display AC activity.



A. Koščíková, J. Černák, L. R. Falvello,  
M. Tomás, I. Ara, J. Titiš, R. Boča

1 – 9

**Cu-Ln ( $\text{Ln} = \text{Gd}, \text{Eu}, \text{Sm}$ ) Dinuclear  
Complexes Based on Schiff Base  
*o-van-en* Ligand: Syntheses, Crystal  
Structures, and Magnetic Properties**

